Tuning the coherent interaction in an on-chip photonic-crystal waveguide-resonator system

Jun Pan,[1,a)] Yijie Huo,[1] Sunil Sandhu,[2] Norbert Stuhrmann,[2] Michelle L. Povinelli,[2,3] James S. Harris,[1] M. M. Fejer,[2] and Shanhui Fan[2]
[1]*Solid State and Photonics Laboratory, Stanford University, Stanford, California 94305, USA*
[2]*E.L. Ginzton Laboratory, Stanford University, Stanford, California 94305, USA*
[3]*Ming Hsieh Department of Electrical Engineering, University of Southern California, Los Angeles, California 90089, USA*

(Received 6 May 2010; accepted 17 August 2010; published online 7 September 2010)

We experimentally demonstrated that the characteristics of the coherent interaction between two waveguide-coupled resonators can be drastically tuned by changing the propagation phase in the waveguide. In particular, the transmission line shape can be tuned between an electromagnetically induced transparency like optical resonance and a flat-top reflection filter. © *2010 American Institute of Physics*. [doi:10.1063/1.3486686]

There has been substantial recent interest in studying coherent interaction and interference between nano-optical resonators. Such studies have led to the experimental demonstrations of all-optical analogs to electromagnetically induced transparency (EIT)[1,2] and super-radiance effects.[3] Efforts along this direction are of fundamental interests since they point to the important conceptual link between atomic physics and nanophotonics. In addition, from a practical point of view, coherent interaction between resonators is important for applications in a large number of on-chip device applications for communications,[4] sensing,[5] and information processing.[6]

In this letter, we consider a photonic-crystal structure in which two resonators are side-coupled to a waveguide (Fig. 1), and experimentally demonstrate that the characteristics of coherent interaction between the two resonators can be drastically tuned by changing the refractive index of the waveguide. As a result, the transmission line shape can be tuned from a flat-top band-reflection filter to an EIT-like line shape and vice versa. Both line shapes are of substantial importance in practical applications. The flat-top band-reflection filter, which reflects a narrow range of wavelengths while letting other wavelengths pass through, is a higher-order filter as compared to the regular Lorentzian line shape commonly observed in photonic-crystal-resonator filters. This filter line shape is important for achieving low interchannel cross-talk in wavelength-division multiplexing and robustness against fluctuations in input-signal wavelength in communication applications.[7,8] The EIT-like optical resonance, on the other hand, renders an integrated optical system transparent at an otherwise highly reflective wavelength. The potential for slowing,[9,10] stopping,[11] and time-reversing of light pulses[12] on chip in such a system has profound impact for both fundamental science and application in optical communication. Our results on tuning therefore experimentally demonstrate substantial reconfigurability as enabled by coherent resonant interactions in these structures. Moreover, in our results, while the EIT line shape has an exact atomic physics analog, the flat-top reflection filter does not. Demonstrating the tuning between these two effects thus indicates some of the unique richness in nanophotonic resonances.

The waveguide-microcavity system in Fig. 1 exhibits various line shapes of transmission spectra depending on the resonant frequency detuning between the two cavities and the propagation phase in the waveguide between them. In coupled mode theory, the normalized power transmission spectrum is[13]

$$|T(\omega)|^2 = \frac{|t_A(\omega)t_B(\omega)|^2}{(1-|r_A(\omega)r_B(\omega)|)^2}\frac{1}{1+4\left(\frac{\sqrt{|r_A(\omega)r_B(\omega)|}}{1-|r_A(\omega)r_B(\omega)|}\right)^2\sin^2\frac{\Phi(\omega)}{2}}, \quad (1)$$

where $t_{A,B}(\omega)$ and $r_{A,B}(\omega)$ are amplitude transmission and reflection coefficients for resonator A, B as follows:

$$t_{A,B}(\omega) = \frac{j(\omega-\omega_{A,B})+\gamma^j_{A,B}}{j(\omega-\omega_{A,B})+(\gamma^c_{A,B}+\gamma^j_{A,B})}, \quad (2)$$

$$r_{A,B}(\omega) = \frac{-\gamma^c_{A,B}}{j(\omega-\omega_{A,B})+(\gamma^c_{A,B}+\gamma^j_{A,B})}. \quad (3)$$

Here, $\omega_{A,B}$ is the resonant frequency of the resonator A or B, γ^j is the intrinsic-loss rate, related to the intrinsic quality factor Q_{int} by $\gamma^j=\pi c/Q_{\text{int}}\lambda_o$, γ^c is the waveguide-cavity coupling rate, related to the coupling quality factor Q_c by $\gamma^c=\pi c/Q_c\lambda_o$, $\Phi(\omega)$ is the total phase accumulated as light goes through a round trip by reflection from both microcavities and propagation in the waveguide $\Phi(\omega)=\phi_A(\omega)+\phi_B(\omega)+\phi_{wg}(\omega)$, where $\phi_{A,B}(\omega)$ is the phase associated with the reflection by the coupled microcavity A or B, $\phi_{A,B}(\omega)=\arg[r_{A,B}(\omega)]$, and $\phi_{wg}(\omega)$ is the round-trip propagation phase in the waveguide, $\phi_{wg}(\omega)=-2\beta(\omega)L$, where $\beta(\omega)$ is the waveguide dispersion relation and L is the spacing between the cavities.

For simplicity we assume two intrinsically lossless resonators with the same coupling rate to a waveguide as follows: $\gamma^j_{A,B}=0$ and $\gamma^c_{A,B}=\gamma$. Coherent interaction between the two resonators occurs only when the two resonators have similar resonant frequencies. In such a case, the transmission line shape is strongly dependent on the propagation phase

a)Electronic mail: panjun@stanford.edu.

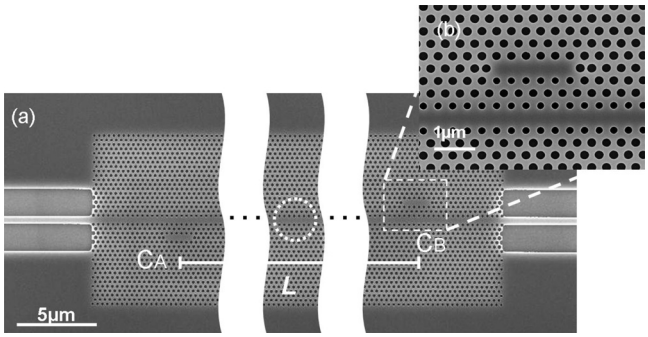

FIG. 1. SEM images of the fabricated device. (a) Top view of the photonic-crystal structure with two cavities side-coupled to one waveguide. (b) Magnified view of the microcavity C_B. The circle approximately corresponds to the size of the focal spot of the pumping laser. The actual heated region however is substantially larger due to thermal conductance.

ϕ_{wg} in the waveguide. As an illustration, we consider in Fig. 2 the cases of $\omega_{A,B}=\omega_0\pm(\delta\omega/2)$, where the reflection phases from the two resonators cancel at ω_0. When $\phi_{wg}(\omega_0)=2n\pi$, the system is therefore on resonance at ω_0, resulting in a transparency resonance peak at ω_0. When $\phi_{wg}(\omega_0)=(2n+1)\pi$, the transparency resonance condition is no longer satisfied. The structure instead behaves as a flat-top reflection filter, which features a much sharper transition between transmission and reflection compared with the single-resonance Lorentzian line shape. As $\delta\omega\to 0$, the transmission spectrum in fact can be simplified as $|T|^2\to[(\omega-\omega_0)^4/(\omega-\omega_0)^4+4\gamma^4]$ which represents a maximum-flat line shape that is of great interest for communication applications.

Motivated by the preceding analysis, we designed a photonic-crystal structure in a suspended silicon membrane with thickness of 320 nm. (Fig. 1) The periodic region consisted of a triangular lattice of air holes with the lattice constant $a=386$ nm, and a hole radius of 116 nm. A single-line-defect waveguide was created by filling one row of air holes. Each resonator was generated by filling five consecutive holes parallel to the waveguide. The nearest hole on either side of the resonator was shifted outward by 77 nm to increase the intrinsic quality factor.[14] The waveguide-resonator

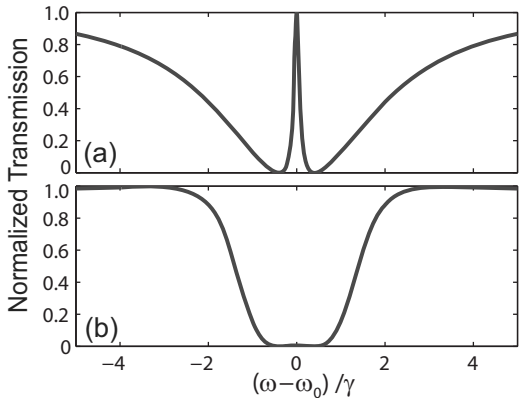

FIG. 2. Graphical illustration of results computed with coupled mode theory. In plotting the curves, we assume two intrinsically lossless resonators with the same coupling rate to a waveguide as follows: $\gamma_{A,B}^i=0$ and $\gamma_{A,B}^c=\gamma$. The resonance frequencies are detuned at an arbitrary small number, $\omega_{A,B}=\omega_0\pm(\delta\omega/2)$, and here we let $\delta\omega=0.8\gamma$. We also assume that the waveguide has a linear dispersion relation $\phi_{wg}(\omega)=-0.2(\omega-\omega_0/\gamma)+\hat{\phi}$. (a) EIT-like transmission spectrum when $\phi_{wg}(\omega_0)=2n\pi$. (b) Flat-top reflection filter when $\phi_{wg}(\omega_0)=(2n+1)\pi$.

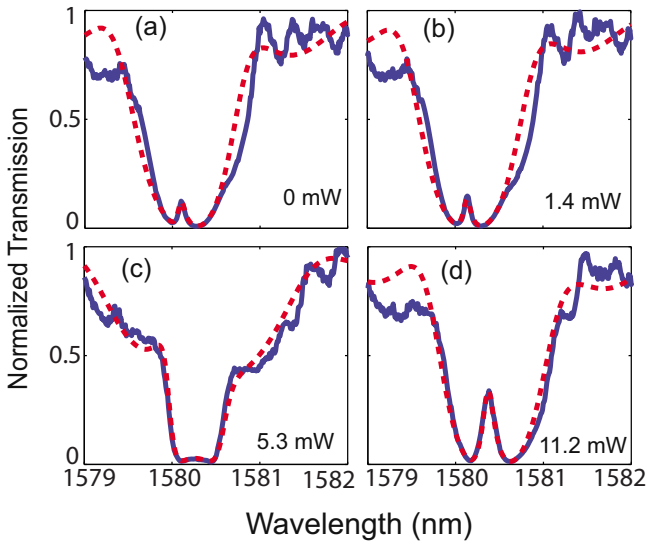

FIG. 3. (Color online) Experimental transmission spectra (blue solid line) and theoretical fits (red dashed line) of the photonic-crystal system of Fig. 1, with a pump laser beam incident on the waveguide near the midpoint between the two microcavities. Curves (a)–(d) correspond to different pump powers. In particular, curves (a), (b), and (d) exhibit a line shape analogous to EIT. Curve (c) exhibits a flat-top reflection response.

coupling occurred through a barrier of three rows of holes. Between the resonator and the waveguide, the radii of the six holes along the side of the resonator and the rows of holes along the side of the waveguide were reduced to 102 nm to enhance the waveguide-cavity coupling. The propagation-phase shift was achieved by laser-pumped thermal tuning on the waveguide. The two resonators were separated by $140a$ in the horizontal direction (L in Fig. 1).

Devices were fabricated on silicon on insulator wafers. The structures were first patterned on poly(methyl methacrylate) by e-beam lithography and transferred to the silicon layer by reactive ion etching. A 1-μm-thick oxide upper cladding was deposited surrounding the strip waveguide. The photonic-crystal membrane was subsequently released by hydrofluoric acid. Finally, the devices were diced from the wafers and the waveguide facets were polished for coupling.

In order to improve coupling and minimize reflections, we incorporated inverse tapers at the ends of the strip waveguide.[15] The width of the strip waveguide in the inverse taper regions gradually decreased from 400 to 150 nm linearly toward the edge of the chip over a distance of 50 μm. In the transmission spectra shown in Fig. 3 that will be discussed in more details below, there are only very weak Fabry–Perot oscillations due to the improved impedance matching at interfaces. The reduction in Fabry–Perot reflections is crucial in order to unambiguously demonstrate the predicted effects that arise from the interference between the two resonators only.

Prior to any tuning, the device exhibited an EIT-like transmission spectrum in Fig. 3(a) featuring a narrow transparency peak in a broad spectral region that had very little transmission. In the subsequent tuning experiments, we focused Ar-ion laser beam with a wavelength of 514 nm into a spot of 2–3 μm in diameter (roughly the circled region in Fig. 1), and gradually increased the pumping power. The heated region however was substantially larger than the laser spot size due to thermal conductance. At a pumping power of 1.4 mW [Fig. 3(b)], the spectrum represented a cleaner EIT-

TABLE I. The parameters used in Eqs. (1)–(3) to fit the experimental curves in Fig. 3. The second column is the power of the laser beam that is delivered to the sample. In the remaining columns the subscripts A or B label the two resonators. $\lambda_{A,B}$ are the resonant wavelengths. $Q_{\mathrm{int},A}$ and $Q_{\mathrm{int},B}$ are the intrinsic quality factors. $Q_{\mathrm{c},A}$ and $Q_{\mathrm{c},B}$ are the waveguide-resonator coupling quality factors. ϕ_0 is a parameter that determines the waveguide propagation phase $\phi_{wg}(\omega)=\tau\omega+\phi_0$, where $\tau=-6.0\times10^{-12}$ s is calculated by the finite-difference time-domain simulation.

Figures	Power (mW)	λ_A (nm)	λ_B (nm)	$Q_{\mathrm{int},A}$	$Q_{\mathrm{int},B}$	$Q_{\mathrm{c},A}$	$Q_{\mathrm{c},B}$	ϕ_0/π
3(a)	0	1580.02	1580.28	13 000	13 000	3900	2200	2524.08
3(b)	1.4	1580.03	1580.29	13 000	13 000	3900	2200	2523.99
3(c)	5.3	1580.09	1580.45	13 000	13 000	3900	2200	2522.76
3(d)	11.2	1580.17	1580.62	13 000	13 000	3900	2200	2521.52

like spectrum as compared with Fig. 3(a); it featured a transparency peak with a higher peak transmission and a near-symmetric line shape. At a pumping power of 5.3 mW, in Fig. 3(c), the EIT-peak disappeared, and we instead observed a flat-top reflection response. At a pumping power of 11.2 mW, the EIT peak was recovered [Fig. 3(d)]. Therefore the experiment has demonstrated the tuning between the EIT and the flat-top response line shapes.

The experimental spectra shown in Fig. 3 are well explained theoretically by Eqs. (1)–(3) with the fitting parameters in Table I. In the experiments, the focused laser beam heats up a portion of the photonic crystal waveguide and the refractive index of silicon increases with temperature by $1.85\times10^{-4}/\mathrm{K}$ at 1.55 μm.[16] The increase in the refractive index pulls the frequency of the guided modes downwards in the band diagram and thereby changes the propagation phase in the waveguide. We assume that the waveguide propagation phase has a linear form $\phi_{wg}(\omega)=\tau\omega+\phi_0$, with $\tau=-6.0\times10^{-12}$ s as determined from the finite-difference time-domain simulation. We further assume that the slope of guided mode band diagram does not change substantially due to the tuning so that τ remains the same, and we vary ϕ_0 to fit the spectra at different tuning powers. Other fitting parameters in Table I are the resonant wavelengths $\lambda_{A,B}$, the intrinsic quality factors $Q_{\mathrm{int},A}$ and $Q_{\mathrm{int},B}$, and the waveguide-resonator coupling quality factors $Q_{\mathrm{c},A}$ and $Q_{\mathrm{c},B}$. The theoretical fit agrees excellently with the experimental measurement.

As an important observation from Table I, all figures are fitted by the *same* set of quality factors. Moreover, both the resonant wavelengths of the two cavities redshift due to the thermal tuning. The detuning between them, however, is kept small enough so that the detuning does not alter the characteristic of the transmission line shape. The change in the line shape, instead, comes almost entirely from the change in the propagation phase ϕ_0. In the spectrum of Fig. 3(c), the round-trip phase at the center of the low-transmission range is close to $(2n+1)\pi$, which is indeed the condition for the flat-top reflection response. On the other hand, the round-trip waveguide phase at transparency peak in Figs. 3(a), 3(b), and 3(d) are all very close to $2n\pi$, the condition of constructive interference in order to generate the EIT-like optical resonance.

A key effect of the EIT-like resonance is the excess group delay.[17] We consider the case of Fig. 3(b) and infer the group delay of the system from the parameters obtained from the theoretical fit. The EIT resonance corresponds to a peak delay of 19 ps, which significantly exceeds the maximum delay of 10 ps as obtained by the sum of the contributions from the two individual resonances and the propagation in the waveguide.

In conclusion, we report the switch of transmission spectrum in a photonic-crystal system between an optical analog to EIT and a flat-top reflection filter. The results demonstrate the substantial flexibility for such photonic-crystal based on-chip devices. Moreover, we have demonstrated that the line shape variation is a result of the change in the propagation phase between the two resonators only, which provides a strong evidence of the coherent nature of the resonant interaction between on-chip resonators.

This work was supported in part by the Slow Light program at DARPA DSO, under the AFOSR Grant No. FA9550-05-0414.

[1] Q. Xu, S. Sandhu, M. L. Povinelli, J. Shakya, S. Fan, and M. Lipson, Phys. Rev. Lett. **96**, 123901 (2006).
[2] X. Yang, M. Yu, D.-L. Kwong, and C. W. Wong, Phys. Rev. Lett. **102**, 173902 (2009).
[3] J. Pan, S. Sandhu, Y. Huo, N. Stuhrmann, M. L. Povinelli, J. S. Harris, M. M. Fejer, and S. Fan, Phys. Rev. B **81**, 041101(R) (2010).
[4] R. Ramaswami and K. N. Sivarajan, *Optical Networks: A Practical Perspective* (Morgan Kaufmann, San Francisco, CA, 1998).
[5] A. M. Armani, R. P. Kulkarni, S. E. Fraser, R. C. Flagan, and K. J. Vahala, Science **317**, 783 (2007).
[6] M. D. Lukin and A. Imamoglu, Nature (London) **413**, 273 (2001).
[7] D. K. Jacob, S. C. Dunn, and M. G. Moharam, Appl. Opt. **41**, 1241 (2002).
[8] Y. Akahane, T. Asano, H. Takano, B.-S. Song, Y. Takana, and S. Noda, Opt. Express **13**, 2512 (2005).
[9] Z. Wang and S. Fan, Phys. Rev. E **68**, 066616 (2003).
[10] A. Yariv, Y. Xu, R. K. Lee, and A. Scherer, Opt. Lett. **24**, 711 (1999).
[11] M. F. Yanik, W. Suh, Z. Wang, and S. Fan, Phys. Rev. Lett. **93**, 233903 (2004).
[12] M. F. Yanik and S. Fan, Phys. Rev. Lett. **93**, 173903 (2004).
[13] L. Maleki, A. B. Matsko, A. A. Savchenkov, and V. S. Ilchenko, Opt. Lett. **29**, 626 (2004).
[14] Y. Akahane, T. Asano, B. S. Song, and S. Noda, Nature (London) **425**, 944 (2003).
[15] S. McNab, N. Moll, and Y. Vlasov, Opt. Express **11**, 2927 (2003).
[16] G. Cocorullo, F. G. C. Della, and I. Rendina, Appl. Phys. Lett. **74**, 3338 (1999).
[17] S. Kocaman, X. Yang, J. F. McMillan, M. B. Yu, D. L. Kwong, and C. W. Wong, Appl. Phys. Lett. **96**, 221111 (2010).